J Seismol (2012) 16:721–731
DOI 10.1007/s10950-012-9306-7

ORIGINAL ARTICLE

Investigation of array-derived rotation in TAIPEI 101

Chin-Jen Lin · Wen-Gee Huang · Han-Pang Huang · Bor-Shouh Huang · Chin-Shang Ku · Chun-Chi Liu

Received: 31 July 2011 / Accepted: 30 April 2012 / Published online: 19 May 2012

Abstract We investigate rotational motions derived from measurements by arrays of translational seismometers—hereafter called array-derived rotations (ADRs)—and compare these to measurements made by a commercially available point rotation sensor (eentec™ R-1™). We focus on two aspects of the array problem: (1) the requisite conditions for calculating an ADR well and (2) the effect of array configuration on the result. Our data set consists of translational accelerations and rotation rates recorded by an array of Kinemetrics™ EpiSensor™ accelerometers and two R-1™ rotational sensors in the TAIPEI 101 building in Taipei, Taiwan. Our results indicate that (1) array configuration affects the accuracy of ADRs about orthogonal components in horizontal plane, (2) coherence between two point rotation measurements (two R-1™) can determine the maximum frequency of translations viably used for the calculating ADRs, and (3) the performance of the R-1™ is adequate, at least above a frequency of 0.12 Hz (periods shorter than 8 s). We also discuss deriving strain from the same array.

Keywords Array-derived rotation · Rotational sensor · TAIPEI 101

C.-J. Lin · W.-G. Huang · B.-S. Huang · C.-S. Ku · C.-C. Liu
Institute of Earth Sciences, Academia Sinica,
128, Sec. 2, Academia Road, Nangang,
Taipei 11529 Taiwan, Republic of China

C.-J. Lin · H.-P. Huang (✉)
Department of Mechanical Engineering,
National Taiwan University,
No. 1, Sec. 4, Roosevelt Road,
Taipei 10617 Taiwan, Republic of China
e-mail: hanpang@ntu.edu.tw

1 Introduction

Rotational ground motions can be measured directly by a rotational sensor ("point" rotations) or by calculations using measurements from a seismic array of translational sensors ("area" rotation, here called array-derived rotations, ADRs). For the former, various techniques for implementing rotational sensors have been attempted, including microelectromechanical systems Coriolis sensors (Nigbor 1994; Takeo 2009), fiber optic gyroscope (FOG; Schreiber et al. 2009; Jaroszewicz et al. 2006), ring laser gyros (RLGs; Schreiber 2005, 2006), Rotaphone (Brokešová and Málek 2010), and molecular electronic technology (MET, Lin et al. 2009; Liu et al. 2009; Wu et al. 2009).

Linear elastic theory indicates that ground rotations can be derived from spatial gradients of translational motions. Two commonly used numerical methods for computing ADRs are a finite difference approximation (Oliveira and Bolt 1989; Huang 2003; Langston 2007) and a geodetic method (Spudich et al. 1995). The prerequisite condition for accurately calculating gradients is that the translational array should be much less than one wavelength. To guarantee this, Langston

(2007) proposed a criterion to determine the maximum frequency of translational data that should be used for calculating those gradients. Until now, no direct evidence has been available to demonstrate this criterion. Here we show that the similarities between rotational waveforms at different locations within the array might provide a way to demonstrate the criterion proposed by Langston (2007).

Comparing rotational waveforms generated by point rotation measurement to those derived from a translational array is of interest both for testing the performance of the rotational sensor and evaluating the ADR technique. Suryanto et al. (2006) were the first to show consistent rotational waveforms between vertical component ADR and point measurements by an RLG; Wassermann et al. (2009) gave the first such comparison for three-axis data sets. However, their results indicate that only the vertical component rotation provides a good waveform match. They did not fully explain the poor comparison between horizontal axis rotation components. Although some studies had been made of the effects of noise on ADRs (Suryanto et al. 2006), little attention has been paid to the influence of rotational axis *orientation*. The axis of rotation computed by ADR is constrained to be perpendicular to the used array plane. In general, ADRs about the vertical axis can be derived well because each horizontal axis translation on the ground can be used to determine vertical axis rotation averagely. However, the orientation of ADRs about a horizontal axis must take into account the array configuration when it is not arranged in an orthogonal shape. In the following section, we investigate this orientation issue with a data set composed of translational and rotational sensors in an array in TAIPEI 101.

2 Deriving rotation from a translational array

The crucial condition for deriving rotation from a translational array is that the strain over the array is spatially uniform (Spudich et al. 1995). Langston (2007) further pointed out that the maximum frequency for computing these spatial gradients of translation is *0.123 c/s* for errors of 10 % or less (c is the wave velocity and s the array aperture) to guarantee that the array aperture is small in comparison to the shortest wavelength analyzed. We propose another method for determining this frequency bound—coherence analysis between two point rotation measurements over the same array. We conclude that the Langston criterion is a reasonable estimate of the maximum frequency of translations that can be used to derive reliable ADRs.

As mentioned, there are two common numerical methods, finite difference method and Spudich's method, for computing ADRs. Since we investigate how array configuration affects the accuracy of ADRs about orthogonal components within the horizontal plane, we prefer to use the simpler method, the finite difference method of Oliveira and Bolt (1989), to derive uniaxial rotation from station pairs, rather than Spudich's method which requires at least three stations to support a least square procedure. The finite difference expression of rotation rate is

$$\dot{\theta}_x = \frac{1}{2}\left(\frac{\Delta\dot{u}_z}{\Delta y} - \frac{\Delta\dot{u}_y}{\Delta z}\right),\quad \dot{\theta}_y = \frac{1}{2}\left(\frac{\Delta\dot{u}_x}{\Delta z} - \frac{\Delta\dot{u}_z}{\Delta x}\right),\quad \dot{\theta}_z = \frac{1}{2}\left(\frac{\Delta\dot{u}_y}{\Delta x} - \frac{\Delta\dot{u}_x}{\Delta y}\right) \tag{1}$$

where $\dot{\theta}_i$ is rotation rate (in radians per second), $\dot{u}_i$ is translational velocity, and the axes are x, y, and z (positive up). A practical numerical calculation can be made simply by differencing two translational records and dividing by the distance between stations.

These difference equations relating translations to rotation are presented in several forms in Table 1 and show that rotation can be derived from translational vectors along the orthogonal direction in the general case (case 1), where the axis of rotation is perpendicular to the translational vectors used. When strain is small compared to rotations and strain gradients are consistent along two orthogonal axes, ADRs can also be derived from parallel translations separated by a distance (cases 2 and 3; Fig. 1b).

We also investigate whether a rotational sensor array can be used to derive shear strain. If the infinitesimal strain approximation is valid, the strain rate $\dot{\varepsilon}_i$ can be represented by

$$\dot{\varepsilon}_x = \frac{1}{2}\left(\frac{\Delta\dot{u}_z}{\Delta y} + \frac{\Delta\dot{u}_y}{\Delta z}\right),\quad \dot{\varepsilon}_y = \frac{1}{2}\left(\frac{\Delta\dot{u}_x}{\Delta z} + \frac{\Delta\dot{u}_z}{\Delta x}\right),\quad \dot{\varepsilon}_z = \frac{1}{2}\left(\frac{\Delta\dot{u}_y}{\Delta x} + \frac{\Delta\dot{u}_x}{\Delta y}\right) \tag{2}$$

Figure 1 illustrates the effect of shear strain and rotation in an infinitesimal block. In pure rotation, gradients along the orthogonal directions are identical, while in shear strain, those gradients have the same amplitude but inverse polarity to one another. Imaging of two separated rotational sensors that are located at

Table 1 Case 1 is the difference equations for deriving rotation rates about three axes from three components of translational velocity

	Case 1	Case 2	Case 3
$\dot{\theta}_x$	$\frac{1}{2}\left(\frac{\Delta\dot{u}_z}{\Delta y}-\frac{\Delta\dot{u}_y}{\Delta z}\right)$	$\frac{\Delta\dot{u}_z}{\Delta y}$	$-\frac{\Delta\dot{u}_y}{\Delta z}$
$\dot{\theta}_y$	$\frac{1}{2}\left(\frac{\Delta\dot{u}_x}{\Delta z}-\frac{\Delta\dot{u}_z}{\Delta x}\right)$	$-\frac{\Delta\dot{u}_z}{\Delta x}$	$\frac{\Delta\dot{u}_x}{\Delta z}$
$\dot{\theta}_z$	$\frac{1}{2}\left(\frac{\Delta\dot{u}_y}{\Delta x}-\frac{\Delta\dot{u}_x}{\Delta y}\right)$	$\frac{\Delta\dot{u}_y}{\Delta x}$	$-\frac{\Delta\dot{u}_x}{\Delta y}$

Cases 2 and 3 are only valid when strain can be neglected in comparison with rigid rotation

an infinitesimal distance apart in a plane is shown in Fig. 1; adding two rotational measurements yields two times the block rotation while subtracting them yields two times the block shear strain. These relations remain valid when strain and rotation occur simultaneously. Although the discussions above are developed for an infinitesimal block (a continuum particle), we believe they are sufficiently accurate for array calculations over a floor slab (e.g., reinforced concrete as in TAIPEI 101) and possibly between floor slabs.

Here we explain why the array's configuration affects the accuracy of ADRs about orthogonal axes in the horizontal plane. Rotation can be seen as a vector, including a magnitude and orientation (normal to the plane of the rotation in a right-handed sense, fingers pointing in the direction of particle motion). If we derive two non-orthogonal rotational vectors $\mathbf{v_1}$ and $\mathbf{v_2}$ from a translational array on the plane, as shown in Fig. 2a, we can still infer orthogonal vectors $\mathbf{u_1}$ and $\mathbf{u_2}$ by using an orthogonalization procedure. Consider the two horizontal plane array configurations in Fig. 2b, c, for example. As in case 2 of Table 1, the horizontal axis rotation can be derived from pairs of vertical axis translation. Considering that the ADR must contain noise like phase uncertainty in the sensors and site variations, the array in Fig. 2c is more effective than the array in Fig. 2b because the array configuration in Fig. 2b increases errors from applying the orthogonalization procedure to nearly parallel axes.

Next we investigate whether the translational measurements need to be corrected for rotational effects, including centrifugal and gravitational accelerations, prior to deriving rotation from them. Seismology is fortunate that centrifugal accelerations induced by ground motion seems small and can be neglected in explosion (Lin et al. 2010) and earthquake records (Lin et al. 2011). For tilt-induced gravitational accelerations acting on the horizontal

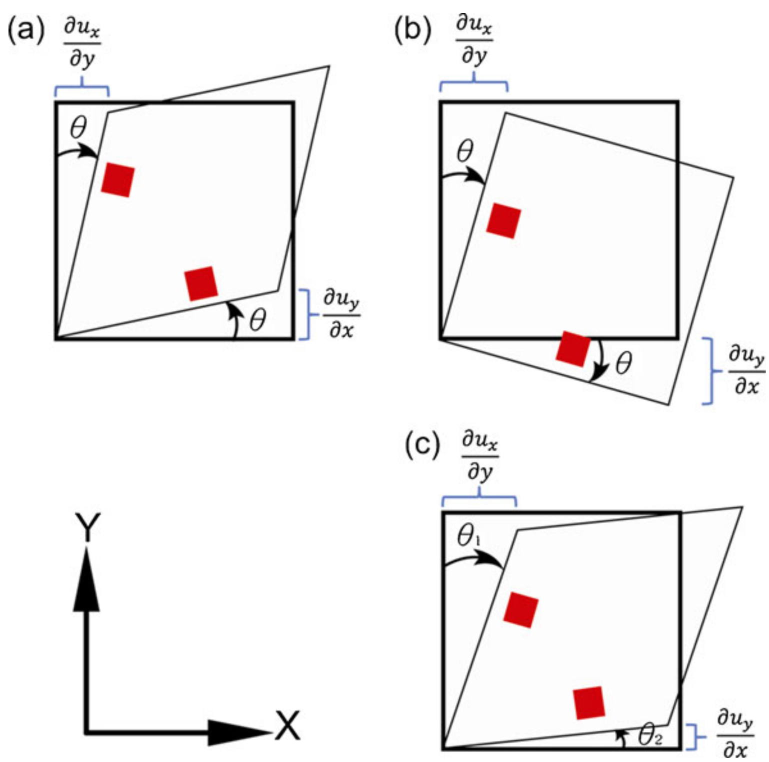

Fig. 1 Deformed and rotating blocks illustrating the effects of **a** pure shear strain, **b** pure rotation, and **c** combined strain and rotation in the *X*–*Y* plane. Strain causes shear deformation while rotation causes rigid rotation. The *red blocks* denote two hypothetical stations providing point rotational measurements about *Z* (deformations are exaggerated for clarity; infinitesimal motions are assumed)

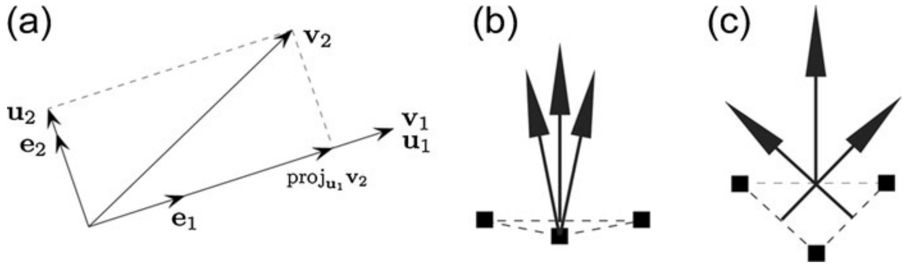

Fig. 2 **a** Two dimensions of the Gram–Schmidt process, while $\mathbf{v}_1$ and $\mathbf{v}_2$ are the known non-orthogonal vectors, **u1** is the same with $\mathbf{v}_1$, $\mathbf{u}_2$ is the vector that $\mathbf{v}_2$ minus its projection onto the $\mathbf{u}_1$, and $\mathbf{e}_1$ and $\mathbf{e}_2$ are the normalized vectors of $\mathbf{u}_1$ and $\mathbf{u}_2$. This orthogonalization procedure is valid for rotation vectors as well. **b**, **c** Two arrays, each composed of three translational stations (*square blocks*) in the horizontal plane, and corresponding horizontal axis rotational vectors (*arrows*) derived from vertical components of these stations

components of the seismometer, because the translational array data has been preprocessed to filter out the high-frequency contents to guarantee that the wavelengths used are larger than the array dimension, tilt effects for long period signal are nearly uniform over an array plane, so they cancel when two translations are differenced.

3 Observations and data processing

The Institute of Earth Sciences, Academia Sinica, Taiwan, started deploying seismic instruments in TAIPEI 101 in 2010. The digitizers in this building are six-channel 24-bit Kinemetrics™ Basalt™. The array is unusual because it includes two three-axis rotational sensors (eentec™ R-1™) in addition to several three-axis translational accelerometers (Kinemetrics™ EpiSensor™). There are four stations in TAIPEI 101; instrument information is summarized in Table 2 and illustrated in Fig. 3. Stations T1S1, T1S2, and T1S3 are located at the southwest corner of TAIPEI 101 at floors B5, 74, and 90 ("B" meaning below ground level). Station T1S4 is located at the northeast corner of TAIPEI 101 at floor 90. This study focuses on the subarray formed by stations T1S2, T1S3, and T1S4 on the 74th and 90th floors.

Since a GPS antenna is difficult to install in a skyscraper like TAIPEI 101, only one station, T1S3, is so equipped. The other three stations (T1S1, T1S2, and T1S4) use Network Time Protocol (NTP) as their time references. Typical time accuracy for internet based NTP is 10 ms with the worst case about 100 ms (for example, section 5.1.3.1 of http://www.ntp.org/ntpfaq/NTP-s-algo.htm#Q-ACCURATE-CLOCK). The sampling rate of our digitizer is 20 samples per second (sps; sampling period is 50 ms), so our instrument configuration is unable to support a wide bandwidth ADR calculation and may increase phase errors due to coarse sampling. However, if the data are filtered to frequencies below 5 Hz (200 ms period), time accuracy should not be a problem.

A six degrees of freedom (DOF) data set from TAIPEI 101 for an Mw 6.9 earthquake northeast of Taiwan in 2011 (epicentral distance of ~498 km; Fig. 4) was gathered. Amplitude Fourier spectra of three axes of acceleration and two of horizontal axis rotation rates at station T1S3 (Fig. 4a) show a fundamental frequency of 0.15 Hz (6.4 s), which is almost the same as the first-mode response of TAIPEI 101 (6.8 s; TAIPEI 101 wind damper website http://www.taipei-101.com.tw/en/DB/index.asp?id=db01). However, vertical axis rotation rate has a higher fundamental frequency of about 0.22 Hz (4.5 s), presumably from a building torsional mode. For translations, waveforms are similar but amplitudes

Table 2 Instrument information for the TAIPEI 101 array

Station	Elevation (floor)	Sensor A	Sensor B	Timing system
T1S1	−22 m (B5)	EpiSensor™	VSE-355 G3™	NTP
T1S2	319 m (74F)	EpiSensor™	VSE-355 G3™	NTP
T1S3	386 m (90F)	EpiSensor™	R-1™ (30s–50Hz)	GPS
T1S4	386 m (90F)	EpiSensor™	R-1™ (20s–20Hz)	NTP

Digitizers are Kinemetrics™ Basalts™ and are continuously recorded at 20 sps. Figure 3 shows approximate station locations within the building

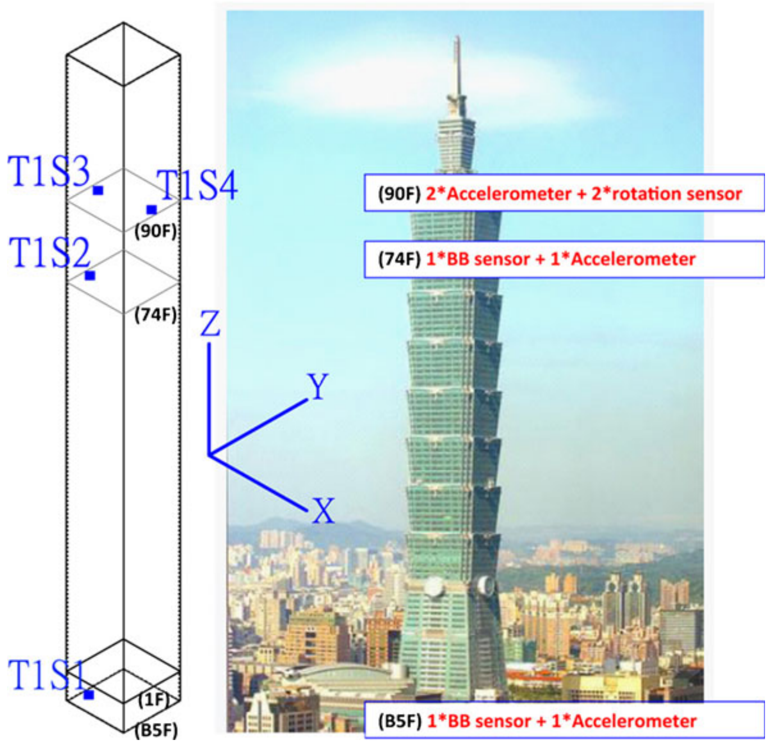

Fig. 3 Schematics of the locations of our seismic stations in TAIPEI 101. A perspective view of stations T1S1, T1S2, T1S3, and T1S4 (*left*). A photo of TAIPEI 101 with sensor information overlaid (*right*). The two horizontal components (*X* and *Y*) are parallel with the sides of the building and the *Z* is vertical. *B5F* fifth floor below ground; *74F* and *90F* floor levels above ground; *BB* a broadband VSE-355G3™ sensor

increase with station elevation. For two rotation rate measurements at the same floor (the 90th; stations T1S3 and T1S4), the waveforms are similar. We infer rotation from the translational array in three ways: (1) we derive vertical axis rotation from horizontal axis translations, (2) derive horizontal axis rotations from translations at different elevations, or (3) on the same plane, and (4) we investigate the maximum frequency of translations that can be used for accurately calculating an ADR.

Before calculating an ADR, we evaluate the criterion presented by Langston (2007) and investigate the similarity between two separated point rotations in the array for comparison. We assume that the shear wave velocity of the steel and concrete floor slabs in TAIPEI 101 is c=3,200 m/s and the largest array aperture is s= 67 m. Therefore, the highest frequency of translation we use to infer rotation should be ~5.9 Hz (0.123× 3200/67). Figure 5 shows coherence results for each point rotation component from stations T1S3 and T1S4. For coherence >0.8, the frequency band for horizontal and vertical components is about 0.12–0.8 and 0.12–3.2 Hz, respectively, so the vertical component has a broader coherent frequency band. This difference is unlikely to the result either from time source errors between the two stations (the Basalt™ digitizers sample all channels simultaneously) nor from signal strength since the amplitudes of the horizontal components are higher than one of vertical components (Fig. 4a). The maximum frequency for uniform strain presented by Langston (2007) of about 5.9 Hz is close to our coherence result for the vertical component but higher than two horizontal components. Whether the coherence result reliably represents the upper frequency limit of ADR computation is discussed below.

In our first experiment, we derive vertical axis rotation from horizontal axis translations on a horizontal plane, a floor slab (Fig. 6a). Referring to the vertical component in case 1 of Table 1, the vertical axis rotation can be derived from the difference between horizontal axis translations divided by separation distances along X and Y. The translational velocity trace is derived from time integration of acceleration and band-pass filtering to the frequency bands discussed above. The Z-axis rotation rate comparison among ADR, and point rotation sensors at T1S3 and T1S4 show good waveform similarity, yielding high zero lag normalized correlation coefficients. This result is our first evidence that high coherence between two rotational sensors over an array can be used to determine the maximum frequency for calculating a viable ADR.

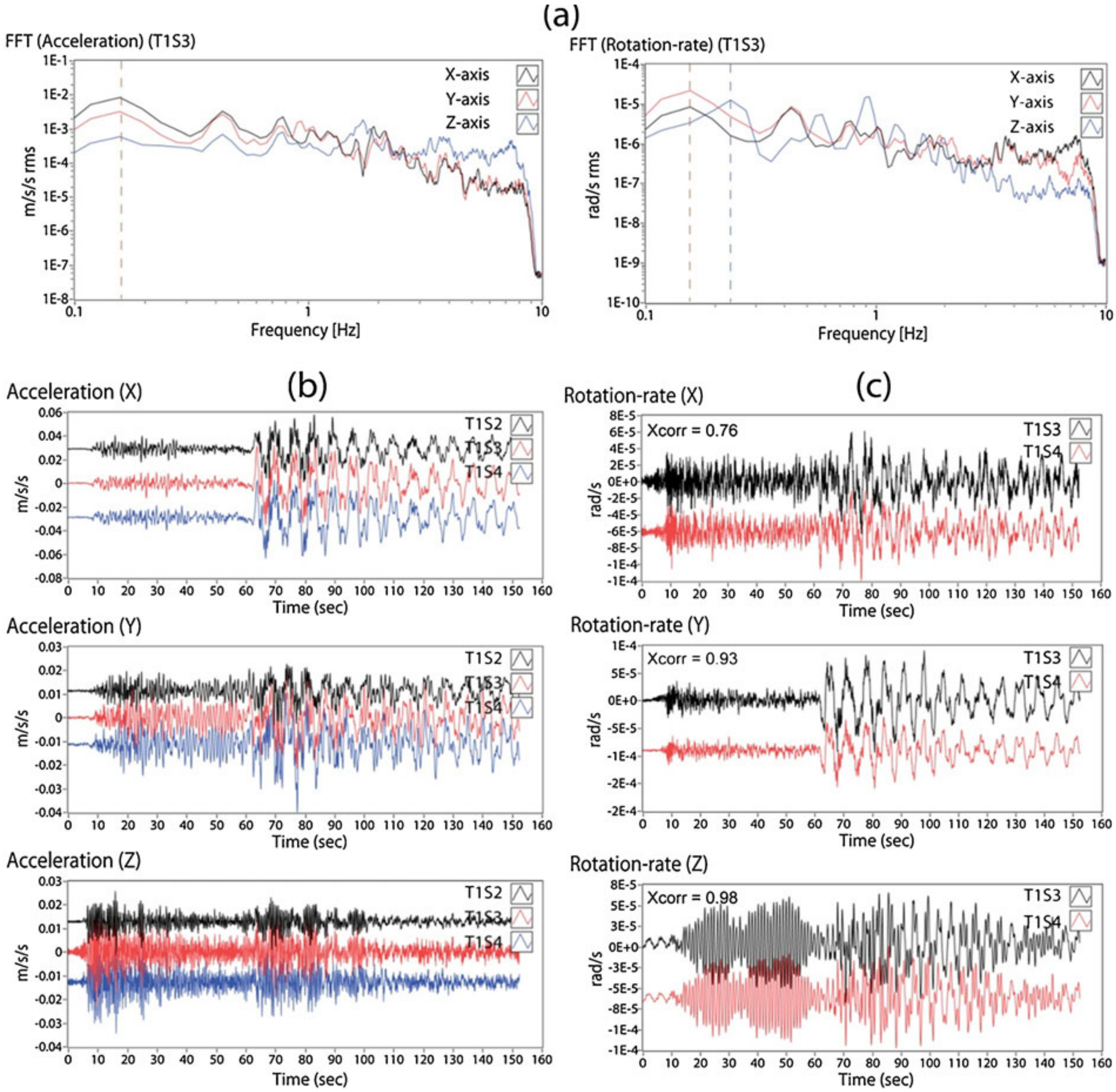

Fig. 4 **a** Amplitude Fourier spectra of acceleration and rotation rate at station T1S3 during an earthquake. The fundamental frequency of the three translations and two horizontal axis rotations is ~0.15 Hz (6.4 s), while the fundamental frequency of vertical axis rotation is ~0.22 Hz (4.5 s). **b** Acceleration traces for stations T1S2, T1S3, and T1S4 without filtering. **c** Point rotation rates for stations T1S3 and T1S4 measured by two R-1™. *Xcorr* zero lag normalized correlation coefficients. Rotation rates waveforms are corrected at mid-band sensitivity only and are not corrected for instrument response. The sensitivities come from laboratory sensor tests (Lin and Liu 2008). All time series are offset for legibility; the *dashed line* represents the fundament frequency

The matched waveform between ADR and two R-1™ measurements also indicates that the performance of the R-1™ is adequate, at least above the frequency 0.12 Hz (periods shorter than 8 s).

In our second experiment, we show that horizontal axis rotation can be derived accurately from stations at different elevations (Fig. 6b, c). Because the relative distances between stations T1S2 and T1S3 along *X*, *Y*, and *Z* are 0.6, 6.73, and 67 m, we simply assume that the stations are located on the *Y*–*Z* plane, ignoring the *X* offset. For the *Y*–*Z* plane in Fig. 6b, translations along *Y* and *Z* are used to derive rotations about *X*

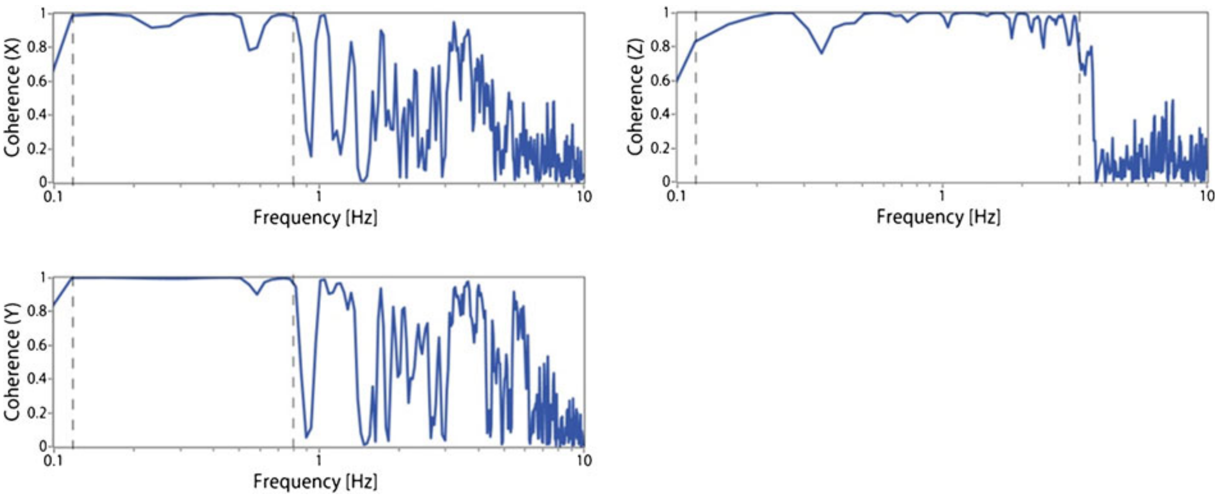

Fig. 5 Coherence of R-1™ point rotation rates about *X*, *Y*, and *Z* between stations T1S3 and T1S4. The *Z* components have a broader frequency band of coherence than the horizontal components (the *dashed line* represents the band with coherence coefficient ≥0.8)

(case 1 in Table 1). The waveform matched well in phase but differs somewhat in amplitude. In Fig. 6c, we ignore the small separation distance along *X* (which would make an *X*–*Z* result prone to errors), so we treat the two stations as if they were directly one above the other (located along *Z*). We assume that interstory strain is small so that the deformation of this subarray can be regarded as a rigid rotation. Therefore, the gradients in translation along *Y* and *Z* directions are consistent and we need use only *X*-axis translations to derive rotation about *Y* (case 3 in Table 1). As before, the waveforms between ADR and R-1™ match well but the amplitudes differ slightly, implying that strain cannot totally be neglected completely in this case.

In our third experiment, we show that horizontal axis rotation also can be derived from stations on a horizontal plane (Fig. 6d) and that the resulting ADR's orientation is perpendicular to a chord between the stations used. Here the shear strain in the vertical plane is taken to be zero (case 2 of Table 1). Because stations T1S3 and T1S4 are not located along *X* or *Y*, the interstation distance is the distance along the chord between them and the result is a rotation vector normal to that chord. In our case, the ADR's orientation is counterclockwise 12.8° from the *Y* (map view) and is denoted as *Y*′. To compare the ADR with an R-1™ measurement, the latter also must be rotated to this orientation. Although the resulting waveforms differ slightly in amplitude (phase is matched well), the comparison still confirms that the orientation of the ADR is perpendicular to the chord. A method for axis transformation of small rotations and rotation rates is provided by Pham et al. (2009a, b); it is effectively the same as translational component coordinate transformation.

Our fourth experiment tests the peak frequency that can be calculated well in an ADR. The coherence result between point rotations at T1S3 and T1S4 stations (Fig. 5) shows that the coherence coefficient for the frequency band of 0.8–3.2 Hz is poor for *X* and *Y* but good for *Z*. In the following, we analyze this frequency band for *Y*′ and *Z* because translations used and the rotational measurements are on the same plane (Fig. 6a, d). Figure 7 is a waveform comparison among ADR, T1S3, and T1S4 and demonstrates that they are adequately similar for rotations about *Z* but poor about *Y*′. This observation is consistent with our previous inference that coherence analysis can be used to estimate the maximum viable frequency of an ADR. We also note that the waveforms are out of phase between measurements of T1S3 and T1S4 for rotation about *Y*′, implying that strain dominates deformation in this instance.

Finally, we investigate whether contrasting rotational measurements over the array can distinguish shear strain from rotation as in our discussion of Fig. 1. An optimal array for the present experiment would have two rotational sensors in each orthogonal plane. Our array configuration does not fulfill this

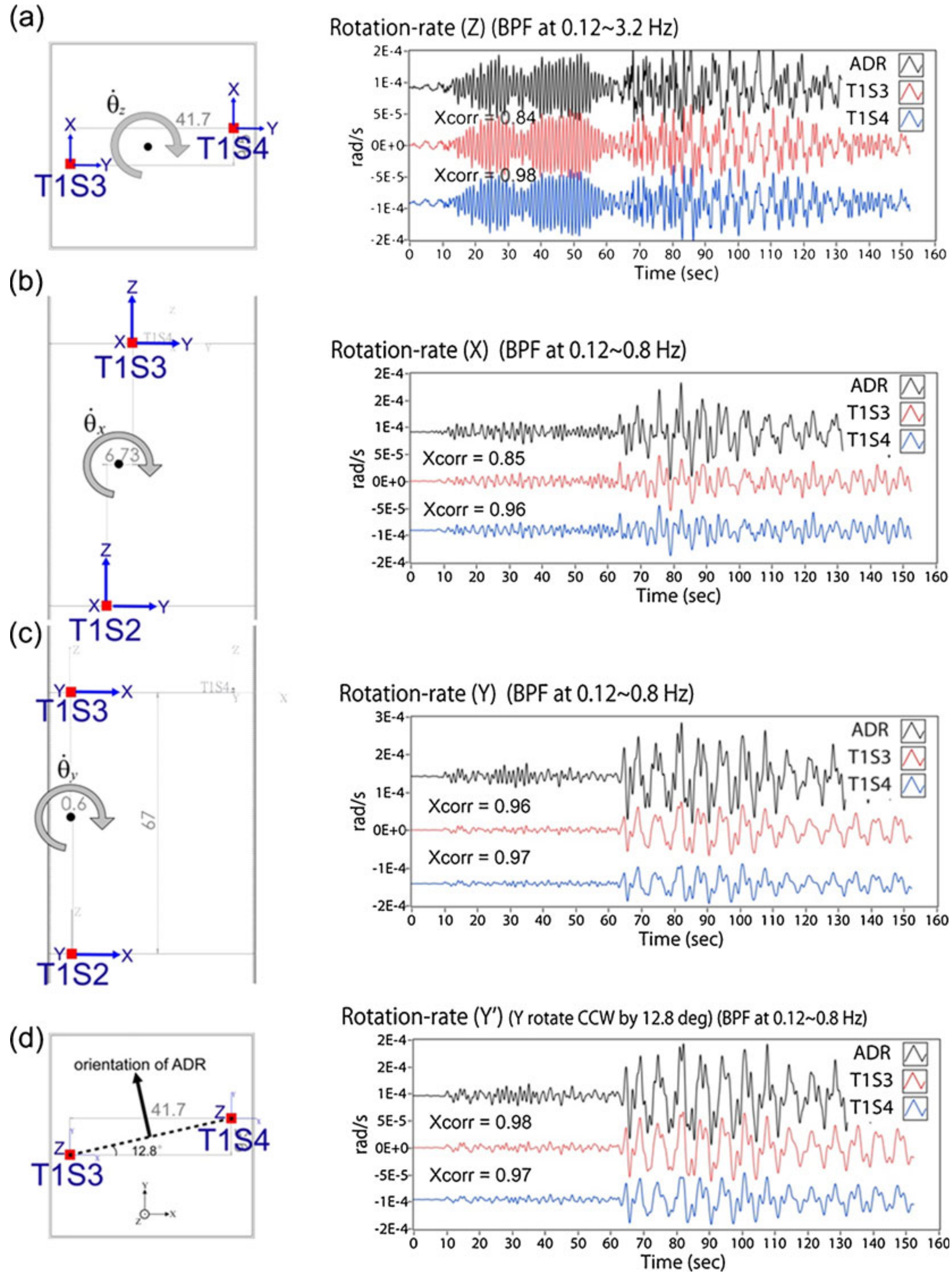

Fig. 6 **a** The *left panel* shows the locations of stations T1S3 and T1S4 in map view (*red blocks*) and their translational acceleration axes (*blue arrows*), as used to calculate an ADR about *Z*. The *right panel* shows the resulting *Z* rotation rate estimate (*black*). Point rotation rates (R-1™) for stations T1S3 and T1S4 are band-pass filtered as discussed in the text. Zero lag normalized correlation coefficients are shown between the ADR and the R-1™ record for stations T1S3, and between the two point rotation measurements, stations T1S3 and T1S4. Waveforms are offset vertically for clarity. **b** Similar to **a** but with stations T1S2 and T1S3 used to calculate the ADR about X. **c** Similar to **b** but for rotations about *Y* computing from *X*-axis translations. **d** The same as **a** except that only *Z* translations are used to derive horizontal axis rotation and the R-1™ records are rotated counterclockwise 12.8° from *Y* to be at the same orientation as the ADR

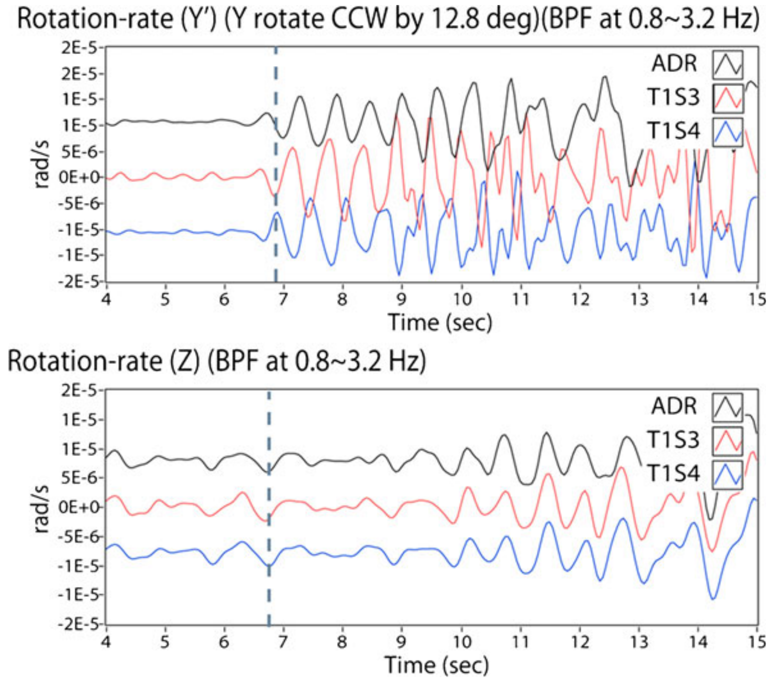

Fig. 7 The P wave portions of waveforms from Fig. 6 filtered to 0.8–3.2 Hz. The *upper panel* waveforms for stations T1S3 and T1S4 are out of phase, so poor coherence. High coherence is evident in the *lower panel* for rotations about Z. The *dashed line* is for the ease comparison only

optimum except for rotation about Z in the $X–Y$ plane; therefore, we assume stations T1S3 and T1S4 are along Y, ignoring the offset along X (Fig. 6a), so that shear strain about X and Z can be derived from the difference of rotational measurement about X and Z. For verifying the viability of this method, we also derive strain from our translational array about X and Z for comparison. Figure 8 shows the strain comparison between these two methods and demonstrates that only the high-frequency P wave shear strains about X have good waveform match, while those about Z do not. The cause of this discrepancy is unclear and requires additional work. Other observations are that (1) the amplitudes of array-derived strains and rotation array differences for the S wave differ significantly and (2) the amplitude of shear strain rate and rotation rate (Fig. 4) is almost of the same order.

4 Discussion and conclusions

We have given evidence that the maximum frequency for reliably calculating an ADR can be determined from coherence between two rotational sensors collocated with the array, and that the result is similar to the criterion proposed by Langston (2007). Our results also indicate that the coherent frequency band for horizontal and vertical components can be different. This variability can be explained easily for buildings because the structure and stiffness of the floor (vertical axis rotation; torsion) and the frame (horizontal axis rotation; tilt) differ. Whether this result appears in ground surface rotations needs further study.

Our result in Fig. 6d demonstrates that horizontal axis rotation can be derived from the vertical axis translations, and that the orientation of the horizontal axis rotation will be normal to the horizontal chord between the stations used. Therefore, if we extend this result to multiple stations on the surface, the accuracy of the horizontal axis rotation is limited by the array configuration due to orthogonalization process, suggesting an explanation for the result of Wassermann et al. (2009) that inconsistent rotation waveforms about horizontal components (between ADR and R-1™ point measurements) arise from the array not being orthogonal. Therefore, we suggest that the translational array should be configured as orthogonal as possible, or at least stations in triangles with equal sides.

Figure 1c suggests that two motion gradients along orthogonal directions are the requisite condition for calculating and distinguishing rotation and shear strain correctly. Our array configuration meets this condition in Fig. 6a and thus has a good waveform match, while Fig. 6b shows somewhat contrasting amplitudes. A possible explanation for this discrepancy in Fig. 6b is

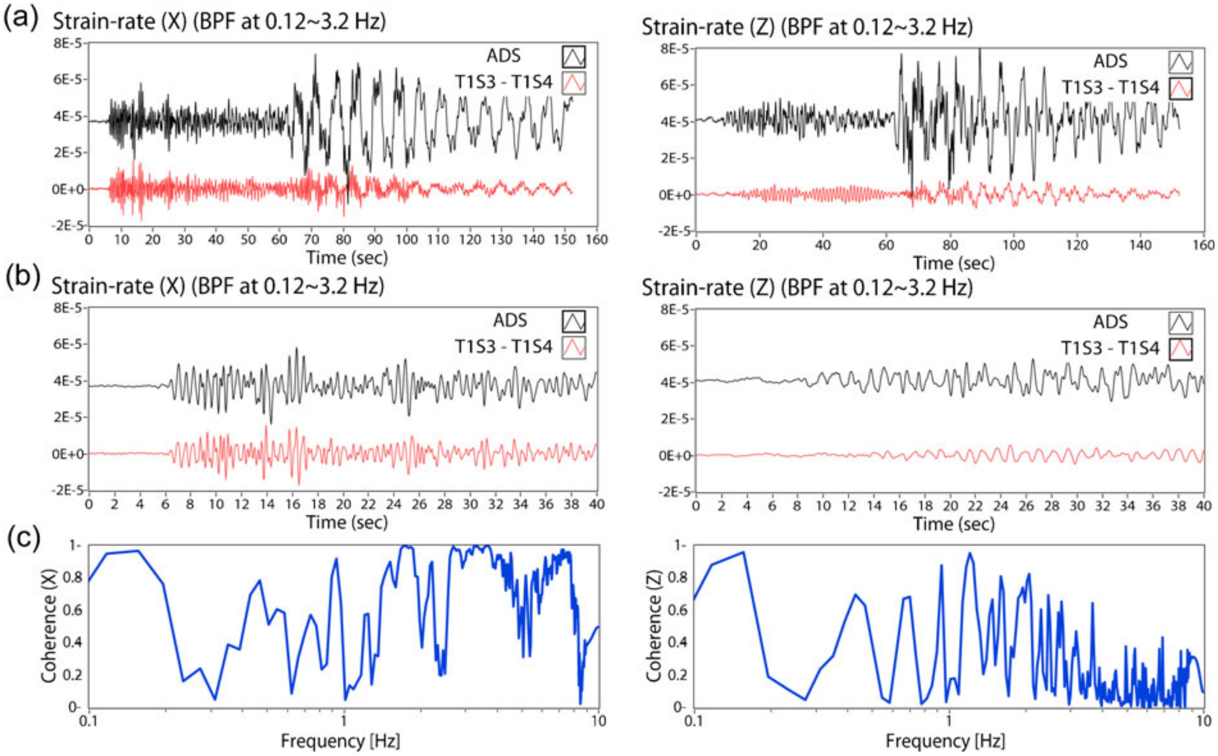

Fig. 8 **a** A comparison of array-derived strain and the difference between T1S3 and T1S4 point rotations about *X* and *Z*. **b** A detail from **a** showing the P wave portion. **c** Coherence between the signals in **a**. *ADS* array-derived strain

that an ADR determines a frame rotation for the *Y–Z* plane between 74F and 90F (with gradients along orthogonal directions), while two point rotational measurements represent the floor rotation in 90F (with gradient along *Y* only; cf. Fig. 1c but with coordinates *X–Y* as *Y–Z*). Our results imply that point rotational measurement on the floor might include contributions from shear strain and cannot directly represent a rigid rotation vector. Whether this result appears in ground surface stations will be studied in the future.

Theory indicates that shear strain can be derived from a translational array or from differential rotational measurements. Unfortunately, we do not observe consistent shear strain waveforms except for the P wave portion about the *X*-axis and that is only somewhat similar. The reason of this discrepancy is an open question; a possible reason cause might be instrumental error in the R-1™ given that Nigbor et al. (2009) show that its frequency response has significant variability between units. Even so, our demonstration indicates that amplitudes of shear strain rate and rotation rate in the skyscraper are in the same order. Strain coherence is worth further investigation for ground surface deformations as well, and we will study deriving ground strain from a combined translational and rotational array in the future.

Finally, Fig. 4a shows a fundamental frequency of vertical axis rotation rate of about 0.22 Hz, which differs from the other five-DOF motions (five degrees of freedom; including two horizontal axis of rotations and three axes of translations). Irwin (2010) suggested that a wind induced vortex around the building's vertical axis might be the major source of *Z* (torsional) rotations in a tall building. Therefore, our results also imply that measuring full six-DOF motions and wind speed in tall building is important.

5 Data and resources

All translational and rotational data analyzed in this paper were collected by the authors with equipment owned by the Institute of Earth Sciences, Academia Sinica, Taiwan. These data have not been released to the public.

Acknowledgments This work was possible because of permission from TAIPEI 101 owners and staff to install the sensors, recorders, and communication system. We are particularly grateful for the marvelous assistance of their Engineering Operation Department. The authors give special thanks to Cathy Yang (vice president of Tower Division), Jeff Sheu (manager), Essen Lin, and Kevin Wu for their support. We would like to sincerely thank John R. Evans and Nguyen Dinh Pham for providing thoughtful reviews and many valuable comments on array-derived rotation. Especially, John R. Evans helped us make this manuscript more readable. We wish to thank editor Johana Brokesova and the three anonymous reviewers for their comments and suggestions that helped to improve the paper.

References

Brokešová J, Málek J (2010) New portable sensor system for rotational seismic motion measurements. Rev Sci Instrum 81. doi:10.1063/1.3463271

Huang B-S (2003) Ground rotational motions of the 1999 Chi-Chi, Taiwan earthquake as inferred from dense array observations. Geophys Res Lett 30(6):1307. doi:10.1029/2002gl015157

Irwin PA (2010) Vortices and tall buildings: a recipe for resonance. Phys Today 63(9):68–69

Jaroszewicz LR, Krajewski Z, Solarz L, Teisseyer R et al (2006) Application of the fibre-optic Sagnac interferometer in the investigation of seismic rotational waves. Meas Sci Technol 17(5):1186

Langston CA (2007) Spatial gradient analysis for linear seismic arrays. Bull Seismol Soc Am 97(1B):265–280. doi:10.1785/0120060100

Lin C-J, Huang H-P, Liu C-C, Chiu H-C (2010) Application of rotational sensors to correcting rotation-induced effects on accelerometers. Bull Seismol Soc Am 100(2):585–597. doi:10.1785/0120090123

Lin C-J, Huang H-P, Pham N, Liu C-C, Chi W-C, Lee W (2011) Rotational motions for teleseismic surface waves. Geophys Res Lett. doi:10.1029/2011GL047959

Lin C-J, Liu C-C (2008) Calibrating the R-1 rotation sensors on CT-EW1 table, vol IESER2008-001. Institute of Earth Sciences Report, Academia Sinica, Taipei, Taiwan

Lin C-J, Liu C-C, Lee WHK (2009) Recording rotational and translational ground motions of Two TAIGER explosions in Northeastern Taiwan on 4 March 2008. Bull Seismol Soc Am 99(2B):1237–1250. doi:10.1785/0120080176

Liu C-C, Huang B-S, Lee WHK, Lin C-J (2009) Observing rotational and translational ground motions at the HGSD station in Taiwan from 2007 to 2008. Bull Seismol Soc Am 99(2B):1228–1236. doi:10.1785/0120080156

Nigbor RL (1994) Six-degree-of-freedom ground-motion measurement. Bull Seismol Soc Am 84(5):1665–1669

Nigbor RL, Evans JR, Hutt CR (2009) Laboratory and field testing of commercial rotational seismometers. Bull Seismol Soc Am 99(2B):1215–1227. doi:10.1785/0120080247

Oliveira CS, Bolt BA (1989) Rotational components of surface strong ground motion. Earthq Eng Struct Dyn 18(4):517–526. doi:10.1002/eqe.4290180406

Pham ND, Igel H, Wassermann J, Cochard A, Schreiber U (2009a) The effects of tilt on interferometric rotation sensors. Bull Seismol Soc Am 99(2B):1352–1365. doi:10.1785/0120080181

Pham ND, Igel H, Wassermann J, Kaser M, de la Puente J, Schreiber U (2009b) Observations and modeling of rotational signals in the P Coda: constraints on crustal scattering. Bull Seismol Soc Am 99(2B):1315–1332. doi:10.1785/0120080101

Schreiber U, Igel H, Cochard A, Velikoseltsev A, Flaws A, Schuberth B, Drewitz W, Müller F (2005) The GEOsensor project: a new observable for seismology. In: Flury RRJ, Reigber C, Rothacher M, Boedecker G, Schreiber U (eds) Observation of the system earth from space. Berlin, Springer, 427–443

Schreiber U, Stedman GE, Igel H, Flaws A (2006) Ring laser gyroscopes as rotation sensors for seismic wave studies. In: Teisseyre MTR, Majewski E (eds) Earthquake source asymmetry, structural media and rotation effects. New York, Springer-Verlag, 377–390

Schreiber KU, Velikoseltsev A, Carr AJ, Franco-Anaya R (2009) The application of fiber optic gyroscopes for the measurement of rotations in structural engineering. Bull Seismol Soc Am 99(2B):1207–1214. doi:10.1785/0120080086

Spudich P, Steck LK, Hellweg M, Fletcher JB, Baker LM (1995) Transient stresses at Parkfield, California, produced by the M 7.4 Landers earthquake of June 28, 1992: observations from the UPSAR dense seismograph array. J Geophys Res 100(B1):675–690. doi:10.1029/94jb02477

Suryanto W, Igel H, Wassermann J, Cochard A, Schuberth B, Vollmer D, Scherbaum F, Schreiber U, Velikoseltsev A (2006) First comparison of array-derived rotational ground motions with direct ring laser measurements. Bull Seismol Soc Am 96(6):2059–2071. doi:10.1785/0120060004

Takeo M (2009) Rotational motions observed during an earthquake swarm in April 1998 Offshore Ito, Japan. Bull Seismol Soc Am 99(2B):1457–1467. doi:10.1785/0120080173

Wassermann J, Lehndorfer S, Igel H, Schreiber U (2009) Performance test of a commercial rotational motions sensor. Bull Seismol Soc Am 99(2B):1449–1456. doi:10.1785/0120080157

Wu C-F, Lee WHK, Huang H-C (2009) Array deployment to observe rotational and translational ground motions along the Meishan Fault, Taiwan: a progress report. Bull Seismol Soc Am 99(2B):1468–1474. doi:10.1785/0120080185